Two-Photon Acid Generation Systems Based on Dibenzylidene Ketone Dyes Intermolecular Sensitization

ARTICLE *in* CHEMISTRY OF MATERIALS · MARCH 2012

Impact Factor: 8.35 · DOI: 10.1021/cm300148n

3 AUTHORS, INCLUDING:

Yuxia Zhao
Technical Institute of Physics and Chemistry
60 PUBLICATIONS **1,125** CITATIONS
SEE PROFILE

Feipeng Wu
Chinese Academy of Sciences
82 PUBLICATIONS **733** CITATIONS
SEE PROFILE

CHEMISTRY OF MATERIALS

Article

pubs.acs.org/cm

Two-Photon Acid Generation Systems Based on Dibenzylidene Ketone Dyes Intermolecular Sensitization

Hao Yuan,[†,‡] Yuxia Zhao,[†] and Feipeng Wu[†,*]

[†]Technical Institute of Physics and Chemistry, Chinese Academy of Sciences, Beijing 100190, P.R. China

[‡]Graduate University of Chinese Academy of Sciences, Beijing 100049, P.R. China

Supporting Information

ABSTRACT: A couple of two-photon absorption dyes containing triphenylamine groups as the electron donor were synthesized. They were combined with commonly used photoacid generator *N*-(trifluoromethanesulfonyloxy)-1,8-naphthalimide (NIOTf) to build two-photon acid generation systems (2PAGs). The photochemical and photophysical properties of these dyes as well as their photosensitizing mechanism were investigated. Both of the two dyes have a greatly enhanced two-photon absorption cross-section over 1000 GM. The photoacid quantum yields of 2PAGs were measured in acetonitrile solution by one-photon process. Fluorescence quenching experiments were carried out and confirmed the electron transfer mechanism in resin films. Also, the acid-catalyzed chemical amplification processes in resin films were studied with a Ti/sapphire regenerative amplifier by attenuated total reflectance Fourier transform infrared spectroscopy, and both 2PAGs exhibited superior efficiencies via two-photon absorption in comparison with isopropylthioxanthone/NIOTf system and NIOTf itself. The two-photon lithography (TPL) was carried out on a Ti/sapphire femtosecond laser system successfully with chemically amplified positive resists based on the achieved 2PAGs and the proceeding power for TPL was as low as 0.24 mW. The results suggest that these 2PAGs can be used as high-efficiency initiator for two-photon chemically amplified positive resist.

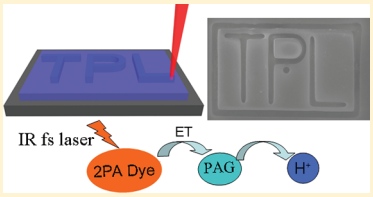

KEYWORDS: *two-photon absorption, chemically amplified positive resist, intermolecular sensitization, two-photon lithography, nonionic photoacid generator*

1. INTRODUCTION

In the photochemical applications focusing on the enhancement of spatial resolution, the two-photon absorption (2PA) process, where a molecule absorbs two photons at longer wavelength simultaneously in the same quantum event, has two advantages over the conventional one-photon process. First, due to the quadratic dependence of 2PA extent on the light intensity, the two-photon process is confined in a small volume around the close vicinity of the laser focus, resulting in high spatial resolution beyond the diffraction limit. Second, in the near-infrared region, the linear absorption of most materials can be neglected, so the laser penetrates into materials without material damage and energy loss out of the focal point. Thanks to these characteristics, many successful works have been carried out in the fields of functional materials, such as three-dimensional microfabrication,[1−3] high-density optical data storage,[4,5] localized photodynamic therapy,[6,7] and two-photon laser scanning fluorescence imaging.[8,9]

Chemically amplified positive resist has been extensively researched since the 1980s.[10−12] The chemical amplification, which means the initial active species catalyze consequent chemical process with a quantum efficiency higher than one, greatly enhances the sensitivity of the positive resist. On the other hand, the acid-catalyzed cleavage process in the positive resist avoids the shrinkage in negative resist based on the free radical polymerization of acrylate family and gives it relatively higher fidelity. Furthermore, in the positive resist, the finally achieved structure is the complement of the exposure pattern; thus, the application of the positive resist would be facile and efficient in certain cases. For instance, it is easier to construct a microfluidic device or a mold for microneedle array by excavating material, rather than curing the whole peripheral structure.

Hence, it is reasonable to say that the application of chemically amplified positive resist in two-photon microfabrication would pave a way for microfabrication with high fidelity and act as a necessary complement to two-photon negative resist. In the development of high-sensitivity two-photon chemically amplified positive resist, the design and preparation of a two-photon acid generator are of critical importance.

One of the strategies to develop the photoacid generator (PAG) for high-sensitivity two-photon chemically amplified positive resist is covalently linking two-photon chromophore and acid-generation functionality together in one molecule. In recent years, several PAGs with enhanced two-photon absorption cross-sections have been successfully synthesized.[3,13,14] However, the challenges in molecular design and the complicated synthesis process limit their further development and wider application.

Received: January 14, 2012
Revised: March 13, 2012
Published: March 14, 2012

dx.doi.org/10.1021/cm300148n | *Chem. Mater.* 2012, 24, 1371−1377

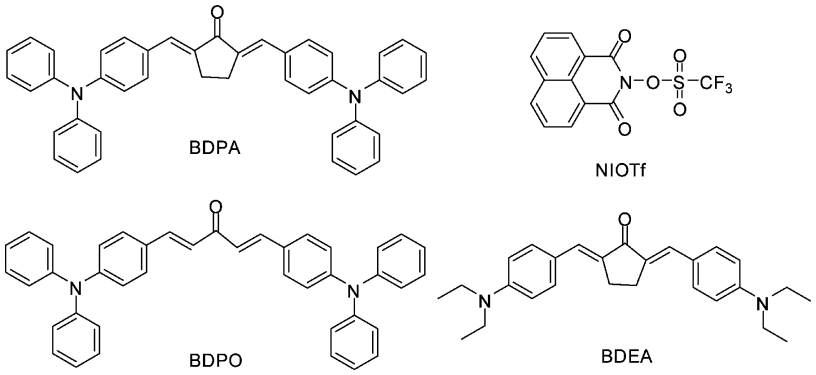

Figure 1. Chemical structures of BDPA, BDPO, BDEA, and NIOTf.

The alternative to high-sensitivity two-photon initiators is intermolecular sensitization systems, where a 2PA dye sensitizes a commonly used UV initiator to generate initial species via a photoinduced electron transfer process. This kind of initiator system has been extensively studied in the negative resist on the basis of free-radical[15−17] and cationic polymerization.[18] It is noteworthy that the concentrations of initiator in common UV chemically amplified positive resists are always relatively high.[19−21] Because the efficiency of the sensitizer in an intermolecular sensitization system is positively correlated with the concentrations of the acceptor, the use of intermolecular sensitization in chemically amplified positive resist may be of more practical superiority. Nevertheless, the application of the intermolecular sensitization is rarely investigated in two-photon chemically amplified positive resist. Lee et al. have demonstrated a two-photon chemically amplified positive resist by using isopropylthioxanthone (ITX) as the photosensitizer,[22] whereas the two-photon absorption cross-section of ITX is too small (σ < 5 GM)[23] to develop a high-sensitivity two-photon acid generation system. To the best of our knowledge, an intermolecular-sensitized acid generation system for a chemically amplified positive resist, which is based on the sensitizer with large two-photon absorption cross-section, has not been reported.

Due to the facile synthesis procedure and the relatively high 2PA cross-section of dibenzylidene ketone dyes, they have attracted considerable attention and have been extensively investigated as highly efficient photosensitizers in two-photo-polymerization.[24−26] However, the commonly used electron donor in these dyes, *N*-alkyl substituted amino groups, would neutralize the photoacid and inhibit the chemical amplification process. We have, herein, synthesized two dibenzylidene ketone dyes containing triphenylamino groups as the electron donor (Figure 1). Since the protonated triphenylamino group is a strong acid (Ph_3N^+H, pK_a = −5),[27] these 2PA dyes would be promising candidates for the photosensitizer that can be applied in chemically amplified positive resist.[3] As the sensitization of ionic PAGs, namely, iodonium salt and sulfonium salt, have been extensively studied,[28−30] the commonly used nonionic PAG *N*-(trifluoromethanesulfonyloxy)-1,8-naphthalimide (NIOTf, Figure 1) is chosen to build the two-photon acid generation systems. By exploiting these two-photon acid generation systems, we demonstrated two-photon lithography (TPL) with typical photopolymer partially *tert*-BOC-protected poly(*p*-hydroxystyrene) (PBOCS) successfully and thereby proved the practice feasibility of the intermolecular sensitization in two-photon chemically amplified positive resist.

2. EXPERIMENTAL SECTION

2.1. Materials. The photoacid generator *N*-(trifluoromethanesulfonyloxy)-1,8-naphthalimide (NIOTf) was synthesized according to the literature.[31] Poly(*p*-hydroxystyrene) was provided by Maruzen Petrochemical Co. Ltd. (Japan). Partially *tert*-BOC-protected poly(*p*-hydroxystyrene) (PBOCS) of 20% protection ratio was synthesized, as described in ref 32. 2,5-Bis[4-(diethylamino)benzylidene]-cyclopentanone (BDEA) was prepared according to the literature procedures.[33] The acid sensor, Rhodamine B base (RBb) was purchased from Acros Organics (U.S.A.). Isopropylthioxanthone (ITX) was obtained from TCI (Japan). All the other reagents were purchased from Beijing Chemical Reagent Company (China) and were used as received without further purification.

2.2. Synthesis of 2,5-Bis[4-(diphenylamino)benzylidene]-cyclopentanone (BDPA). The 4-formyltriphenylamine was synthesized by Vilsmeier−Haack reaction from triphenylamine.[34] 0.54 g (2 mmol) of 4-formyltriphenylamine, 0.084 g (1 mmol) of cyclopentanone, and 35 mL ethanol were mixed in a three-neck flask. After the addition of the catalyst (NaOH 0.04 g), the flask was flushed with nitrogen, and the mixture was heated to 70 °C for 2 h. After cooling, the orange crystal was filtered and purified by column chromatography using dichloromethane as eluent. Yield: 0.56 g (90%). ^{1}H NMR (400 MHz, $CDCl_3$) δ 7.56 (s, 2H), 7.47 (d, J = 8.8 Hz, 4H), 7.34 − 7.27 (m, 8H), 7.15 (d, J = 7.5 Hz, 8H), 7.10 (t, J = 7.3 Hz, 4H), 7.05 (d, J = 8.7 Hz, 4H), 3.06(s, 4H). HRMS: Calc. for $C_{43}H_{34}N_2O$, m/z 594.2671, found m/z 594.2640. Elem. Anal. calcd. for $C_{43}H_{34}N_2O$: C, 86.84; H, 5.76; N, 4.71. Found: C, 86.91; H, 5.77; N, 4.70.

2.3. Synthesis of 1,5-Bis[4-(diphenylamino)phenyl]penta-1,4-dien-3-one (BDPO). 0.54 g (2 mmol) of 4-formyltriphenylamine and 30 mL ethanol were mixed in a three-neck flask. After the addition of the catalyst (NaOH 0.04 g), the flask was flushed with nitrogen, and the mixture was heated to 60 °C. Over a period of 30 min, 0.058 g (1 mmol) acetone in 10 mL ethanol was added dropwise. Two hours later, the reaction mixture was cooled to room temperature, and the solvent was removed with rotary evaporator. Afterward, the resulting residue was separated by column chromatography using dichloromethane as eluent. Yield 0.26 g (45%). ^{1}H NMR (400 MHz, $CDCl_3$) δ 7.71 (d, J = 15.8 Hz, 2H), 7.48 (d, J = 8.7 Hz, 4H), 7.36 − 7.29 (m, 8H), 7.16 (dd, J = 7.5 Hz, 8H), 7.12 (d, J = 7.4 Hz, 4H), 6.96 (d, J = 15.8 Hz, 2H). HRMS calcd. for $C_{41}H_{32}N_2O$: m/z 568.2515. Found: m/z 568.2520. Elem. Anal. calcd. for $C_{41}H_{32}N_2O$: C, 86.59; H, 5.67; N, 4.93. Found: C, 86.75; H, 5.66; N, 4.90.

2.4. General Characterization. UV−vis absorption spectra were recorded on a Hitachi U3900 spectrophotometer. Fluorescence spectra were obtained using a Hitachi F-4500 spectrometer. Fluorescence quantum yields were measured in diluted solutions by utilizing Fluorescein in 0.1 M NaOH aqueous as the reference (Φ = 0.9).[35] ^{1}H NMR spectra were obtained on a Bruker Avance-DPX400 spectrometer. The HRMS analyses were carried out on a Waters GCT Premier mass spectrometer. Elemental analyses were performed on a Flash EA 1112 elemental analyzer. The fluorescence lifetime τ was measured by single photon counting method using an Edinburgh FL920 spectrometer. The measurements of the two-photon absorption

dx.doi.org/10.1021/cm300148n | *Chem. Mater.* 2012, 24, 1371−1377

cross-section and photoacid generation quantum yield are presented in the Supporting Information.

2.5. Electrochemical Experiments and Free Energy Changes of Photoinduced Electron Transfer. The reduction and oxidation potentials of the compounds were measured by cyclic voltammetry. A trielectrode system was used for measurements with a Ag/Ag^+ reference electrode, a platinum rod counter electrode, and a platinum plate working electrode. All measurements were carried out in N_2-saturated acetonitrile containing 0.1 M of tetrabutylammonium hexafluorophosphate as the supporting electrolyte at a scan rate of 100 mV/s. All potential values were estimated from half-peak potentials and converted to the potentials versus SCE by using ferrocene as an internal standard.

The free energy changes of the photoinduced electron transfer from the excited sensitizers to NIOTf were calculated from the Rehm–Weller equation[36] as follows:

$$\Delta G_{ET}\ (\text{kcal mol}^{-1}) = 23.06\left(E_{ox} - E_{red} - \frac{e_0^2}{a\varepsilon} - E_{00}\right) \quad (1)$$

where E_{ox} and E_{red} are the oxidation potential of the sensitizer and the reduction potential of NIOTf, respectively. The E_{00} is the excited state energy of the photosensitizer, which was obtained from the wavelength of intersection of the normalized absorption and emission spectra (E_{00} in PBOCS film was determined in the same way). $e_0^2/a\varepsilon$ is the energy obtained when two free ions reach distance a in the solvent with a dielectric constant of ε (0.06 eV in acetonitrile).[37]

2.6. Photoacid Generation and Chemical Amplification in Resin Films by 2PA. Chemically amplified positive resists A, O, E, I, and R were prepared with typical photoresist polymer PBOCS using diethylene glycol dimethyl ether (DGDE) as the solvent. The components of these resins were listed in Table 1. After spincoating the resin on a glass-slide, the film was baked at 110 °C for 60 s. Independent samples were exposed to femtosecond laser from Ti/sapphire regenerative amplifier (Spitfire, Spectra-Physics, 1000 Hz, <130 fs, 800 nm) at different times, and then, the post exposure bake process was applied on a thermostatic hot plate at 110 °C for 60 s. The attenuated total reflection Fourier transform infrared spectra (ATR-FTIR) of the exposed resin films were obtained on an Excalibur 3100 infrared spectrophotometer.

Table 1. Components of Resins Used in the Chemical Amplification Measurement and TPL

		component (wt %)			component (mol kg^{-1})	
resin	initiator system	PBOCS	sensitizer	NIOTf	sensitizer	NIOTf
A	BDPA/NIOTf	94	1	5	0.017	0.145
O	BDPO/NIOTf	94	1	5	0.017	0.145
E	BDEA/NIOTf	94.3	0.7	5	0.017	0.145
I	ITX/NIOTf	94.7	0.3	5	0.017	0.145
R	NIOTf	95	none	5	none	0.145

In the post exposure bake procedure, *t*-BOC groups were cleaved by the catalysis of photoacid, resulting in the decrease of the carbonyl band at 1730 cm^{-1} in ATR-FTIR spectra. As the concentration of benzene ring in resin films was constant, the deprotection extent was calculated from the height of the carbonyl band by using the band of benzene ring at 1510 cm^{-1} as the internal standard.

2.7. Two-Photon Lithography. TPL was carried out using resins A and O. A mode-locked Ti/sapphire laser (Tsunami, Spectra-Physics, 80 MHz, 100 fs, 780 nm) was tightly focused via an oil-immersion objective lens (100×, NA = 1.4, Olympus) into the sample. The focal spot was scanned on the *x*–*y*-plane by a two-galvano-mirror set (HurrySCAN 14, SCANLAB), and along the *z*-axis by a piezostage (P-622.ZCL, PI). The laser power applied to the resin film was measured on the front of the objective lens. Except for the exposure process, the other process flow was the same as that in section 2.6. After the post exposure bake, the sample was developed in aqueous 0.26 M tetramethylammonium hydroxide (TMAH) for 5 s and rinsed with deionized water immediately. The obtained microstructures were characterized by SEM (Hitachi S-4300FEGd).

3. RESULTS AND DISCUSSION

3.1. Photophysical Properties. The UV–vis absorption spectra and steady-state fluorescence spectra of BDPA and BDPO are reported in Figure 2. The results of the absorption and fluorescence measurements were summarized in Table 2.

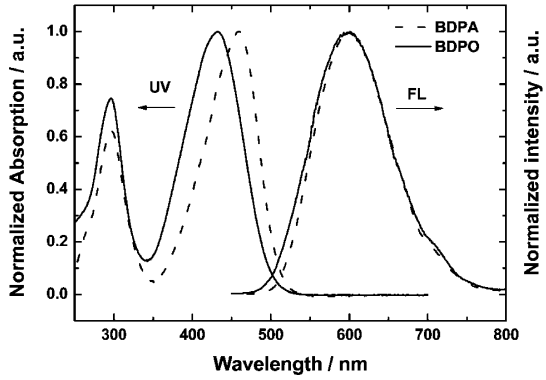

Figure 2. Normalized absorption and emission spectra of BDPA (dashed) and BDPO (solid) in acetonitrile.

The two compounds consist of a typical D–π–A–π–D structure, where the triphenylamino, vinyl, and carbonyl groups were employed as donor (D), π-conjugated center (π), and acceptor (A) moieties, respectively. Like the other dibenzylidene ketone dyes, both BDPA and BDPO had a strong charge transfer (CT) absorption band at 400–500 nm and a typical localized absorption band of triphenylamino group around 300 nm. The CT absorption band of BDPA was located at 459 nm and that of BDPO was blue-shifted to 433 nm, probably because the cyclopentanone linkage gave BDPA a relatively higher molecular rigidity as well as a higher degree of conjugation compared to BDPO. Despite the difference in the absorption spectra, the emission spectra of the two dyes almost showed the same peak position and shape in acetonitrile. The measured fluorescence quantum yields of BDPA and BDPO were 0.050 and 0.027, respectively, indicating the higher molecular flexibility of BDPO led to stronger nonradiative deactivation of the excited singlet state.

The two-photon absorption (2PA) spectra were measured over a wavelength range of 710–880 nm. The quadratic relationship between the fluorescence intensity and the excitation power confirms the two-photon absorption process (Supporting Information, Figure S3, S4). The σ values of two compounds were calculated and presented in Figure 3. The 2PA maxima of BDPA and BDPO were located at 820 and 760 nm, respectively, showing remarkable blue-shift compared to the double wavelength of their linear absorption peaks. This means that some higher excited states with different parity are reached by 2PA with respect to one-photon absorption.[16] Compared with the typical dibenzylidene ketone 2PA dye BDEA (Figure 1), the higher 2PA cross-section found in BDPA might be due to the extended π-conjugated system resulting from the introduction of triphenylamino groups.[38] On the other hand, BDPO, which bears triphenylamine groups as well, shows a relatively lower 2PA cross-section, likely because of the

dx.doi.org/10.1021/cm300148n | *Chem. Mater.* 2012, 24, 1371–1377

Table 2. Relevant Photochemical and Photophysical Properties of BDPA and BDPO[a]

cmpd	λ^{abs} (nm)	λ^{fl} (nm)	$\Delta\nu_{ss}$ (cm^{-1})	Φ_{fl}	τ (ns)	σ_{max} (GM)	E_{ox} (eV)	$E_{00}{}^{a}$ (eV)	ΔG_{et} (kcal mol^{-1})	Φ_H	k_q (L M^{-1} s^{-1})	$E_{00}{}^{b}$ (eV)	R_q (Å)
BDPA	459	600	5119	0.05	1.2	1310	0.93	2.41	−12.2	0.009	1.30×10^{10}	2.27	6.4
BDPO	433	600	6428	0.027	0.75	1049	0.94	2.47	−13.4	0.053	1.38×10^{10}	2.42	8.0

[a] $\Delta\nu_{ss}$ is Stoke's shifts; τ is the fluorescence lifetime; σ_{max} is the maximum 2PA cross-section obtained within 710−880 nm; k_q is the fluorescence quenching constant in acetonitrile solution; $E_{00}{}^{a}$ is the energy of excited singlet state in acetonitrile solution; $E_{00}{}^{b}$ is the energy of excited singlet state in PBOCS film.

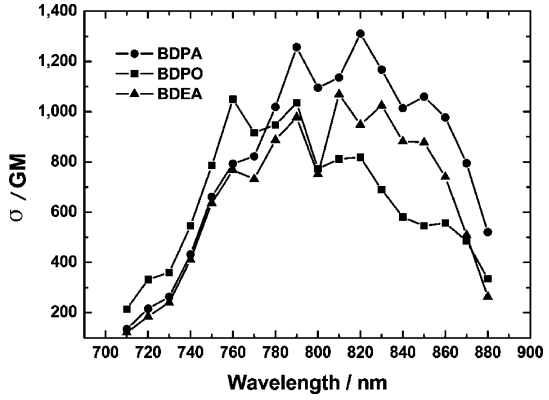

Figure 3. Two-photon excitation spectra for BDPA, BDPO, and BDEA in acetonitrile solution.

relatively poorer conjugation degree coming from the supple acetone-linkage.

3.2. Electron Transfer in the Dye-Sensitized Photoacid Generation System. The synthesized two-photon sensitizer BDPA and BDPO were combined with the photoacid generator *N*-(trifluoromethanesulfonyloxy)-1,8-naphthalimide (NIOTf), respectively, to build a dye-sensitized photoacid generation system. As the sensitizer was excited by a one-photon process or a two-photon process, one electron transferred from the excited sensitizer to NIOTf in the ground state. The resulting radical anion of NIOTf then cleaved and reacted with the trace water in the polymeric media as well as in net acetonitrile (0.003 wt %)[39] to generate trifluoromethanesulfonic acid.[40]

By cyclic voltammetry, the oxidation potentials E_{ox} of BDPA and BDPO were measured to be 0.93 and 0.94 V (vs SCE) respectively (Supporting Information, Figure S1). The reduction potential E_{re} of NIOTf was −1.01 V (vs SCE). The free energy changes of the photoinduced electron transfer from the excited sensitizers to NIOTf were calculated from the Rehm−Weller equation (see eq 1 in the Experimental Section). The calculated ΔG_{et} (listed in Table 2) indicates that both of the dye/NIOTf systems possess a favorable thermodynamic driving force ($\Delta G_{et} < -10$ kcal mol^{-1}) upon exposure to light. It means that the photoinduced electron transfer will proceed spontaneously from the excited singlet state of the sensitizer to the ground state of NIOTf. These results coincide with the fact of the dynamic fluorescence quenching experiment in acetonitrile, where the fluorescence of BDPA and BDPO was effectively quenched by the addition of NIOTf. Both of the values k_q are close to the diffusion-controlled limit in acetonitrile (Table 2).[30]

3.3. Photobleaching and Photoacid Generation in Solution by One-Photon Process. The N_2-saturated solutions containing the same concentration of the sensitizers and NIOTf were exposed to 473 nm CW semiconductor laser at different durations, and then, the same volume of RBb stock solutions were added to the solutions. In both dye/NIOTf pairs studied, the solution acidity increased over irradiation time, and so, the characteristic absorbance at λ_{max} (555 nm) of Rhodamine B base increased correspondingly (Figure 4).

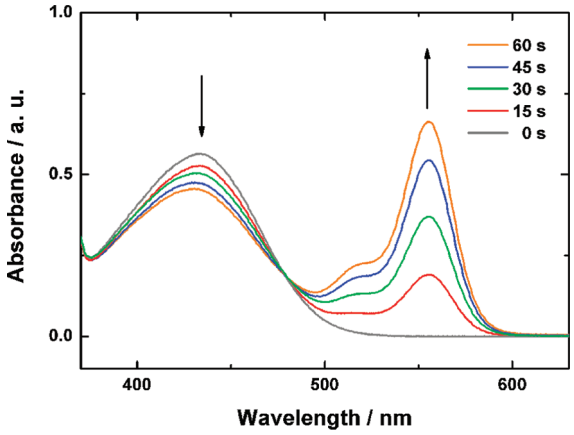

Figure 4. Relationship between photobleaching of BDPO and photoacid generation. Independent mixed solutions of BDPO (1×10^{-5} M) and NIOTf (1×10^{-3} M) in acetonitrile were irradiated at different times (0, 15, 30, 45, and 60 s). The concentration of RBb was 1×10^{-5} M.

Meanwhile, the photobleaching of the absorbance of sensitizers (433 nm for BDPO) were observed. Additionally, in the control experiment, the photolysis of the dyes alone did not generate any acid. These results confirmed that both the dye-sensitized photoacid generation systems could generate acid by photo-induced electron transfer process.

The calculated quantum yields of photoacid generation Φ_H are presented in Table 2. The concentration of NIOTf in this measurement was fixed up to 1×10^{-2} M in order for the dynamics factors involved in the photoacid generation process to be minimized. However, according to the quenching constant obtained in the dynamic fluorescence quenching experiments, even at this concentration of NIOTf, no more than 15% of the excited singlet states of the sensitizer were quenched. That is to say, although it is more favorable in terms of thermodynamic driving force, the electron transfer from excited singlet state of the sensitizer does not account for the main contribution to the acid generation in acetonitrile solution.

To verify the role that the excited triplet state of sensitizers played in the photoacid generation process, the influence of the well-known triplet quencher, anthracene (energy of lowest triplet state: 177 kJ mol^{-1}), on the photoacid generation was investigated. As different amount of substances of anthracene were added to several identical sensitizer/NIOTf solutions respectively, the fluorescence intensity of these solutions did not change with the addition of anthracene. This proved that

dx.doi.org/10.1021/cm300148n | *Chem. Mater.* 2012, 24, 1371−1377

the addition of anthracene did not increase the deactivation of singlet excited state of the sensitizer. As shown in Figure 5, at

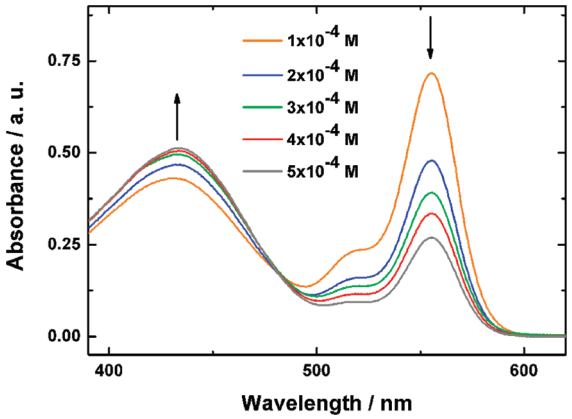

Figure 5. Influence of the addition of anthracene on photoacid generation. The mixed solutions of BDPO (1×10^{-5} M) and NIOTf (1×10^{-3} M) with different concentrations of anthracene were irradiated at the same irradiation dose. The concentration of RBb was 1×10^{-5} M.

the same exposure dose, the photoacid generated in these solutions decreased gradually with the increase of the concentration of anthracene. The inverse correlation between the photoacid generation and the concentration of anthracene revealed the possibility that the electron transfer between the sensitizer and NIOTf occurred via the triplet state. In solution, where the electron transfer was controlled by diffusion process, intermolecular sensitization often proceeded via excited triplet states of sensitizer rather than the singlet states of shorter lifetime. This phenomenon is often reported in the studies of dye-sensitized initiator system.[30,41]

3.4. Fluorescence Quenching in Resin Films. To understand the electron transfer process in resin film, a fluorescence quenching experiment was carried out in spin-coated film, where the fluorescence intensity of the sensitizer was found to decrease with the addition of NIOTf. Contrary to Stern–Volmer kinetics, which describes the dynamic fluorescence quenching process in solution and takes the diffusion into account, the Perrin equation (eq 2) describes the fluorescence quenching process that takes place between immobilized fluorescent substance and quencher molecules.

$$\ln(I_0/I) = VN_AC_q \quad (2)$$

where I_0 is the fluorescence intensity in the absence of the quencher, I is the observed fluorescence intensity relative to the quencher concentration, N_A is Avogadro's number, C_q is the concentration of the quencher, and V is the volume of the "quenching sphere". The quenching radius R_q is calculated correspondingly and presented in Table 2.

As shown in Figure 6, the data of fluorescence quenching experiment fitted eq 2 reasonably well. Since the Perrin equation was deduced on the premise that the fluorescent substance and quencher molecules distributed randomly in solid phase as in solution, the results indicated that there was no complex formed between the sensitizer and NIOTf in resin films and NIOTf itself did not aggregate or crystallize in this range of concentrations.[42] The calculated quenching radius of BDPO (R_q = 8.0 Å) was larger than that of BDPA (R_q = 6.4 Å).

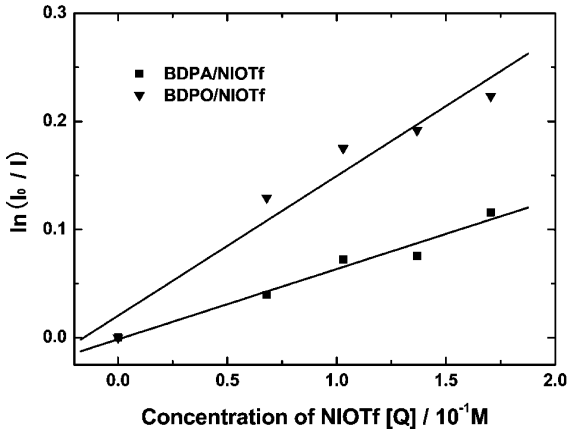

Figure 6. Relative intensity of the fluorescence of BDPA and BDPO with the addition of NIOTf in resin films.

This indicated that NIOTf could quench the excited singlet state of BDPO with relatively higher efficiency in PBOCS films.

Additionally, the absorption and emission spectra were obtained in PBOCS films (Supporting Information, Figure S2) and gave an E_{00} value of BDPA and BDPO of 2.27 and 2.42 eV, respectively. It has been reported that the quenching radius correlated with free-energy change of the electron transfer in a polymer solid matrix.[42−44] So, BDPO with a higher E_{00} value reasonably showed a larger R_q.

3.5. Photoacid Generation and Chemical Amplification in Resin Films by 2PA. In two-photon microfabrication, the incident laser beam was tightly focused into a subwavelength tiny volume. Therefore, the consequent chemical and physical processes initiated by 2PA were limited in this small range. For this reason, it was difficult to directly monitor the reaction initiated by 2PA in resin films. Generally speaking, for two-photon negative-tone photoresist, the sensitivity of an initiator system was evaluated in terms of energy threshold for two-photon microfabrication. However, for two-photon chemically amplified positive photoresist, the acid-catalyzed chemical amplification did not finish instantaneously after the exposure and the time interval from the exposure to the post exposure bake influenced the measurement of the energy threshold. Additionally, the process of development imparted non-negligible discrepancy to the results of energy threshold as well. Here, to evaluate and compare the efficiencies of different initiator systems, we applied a methodology that took advantage of a Ti/sapphire regenerative amplifier to initiate 2PA in a detectable area. The intensity of this femtosecond laser satisfied the energy requirement of 2PA and the diameter of the light beam made the spot where the photoreaction took place large enough for ATR-FTIR measurement.

In this method, photoacid generation by 2PA in resin film was investigated by measuring the acid catalyzed deprotection of PBOCS after exposure to the femtosecond laser from the regenerative amplifier. As shown in Figure 7, the deprotection extents were plotted against irradiation time to estimate the efficiencies of the two two-photon acid generation systems in comparison with NIOTf itself and ITX/NIOTf. On exposure to near-IR femtosecond laser, ITX did not exhibit remarkable sensitizing efficiency, and the deprotection extent of ITX/NIOTf sample was almost the same as that of the sample containing NIOTf alone. Both BDPA and BDPO showed significant sensitizing efficiencies. It is noteworthy that BDPA

dx.doi.org/10.1021/cm300148n | Chem. Mater. 2012, 24, 1371−1377

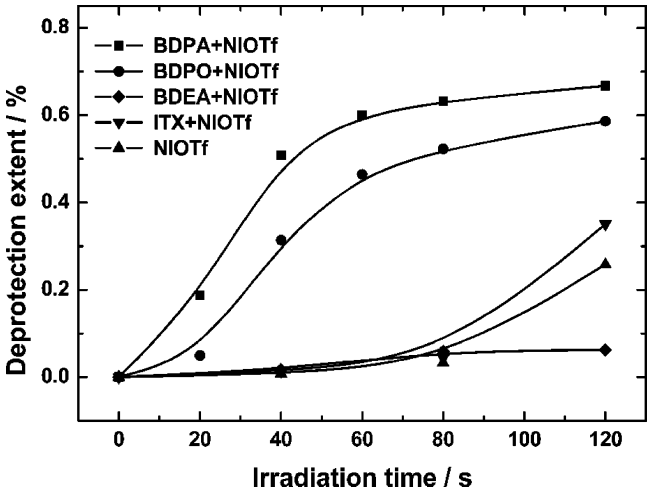

Figure 7. Deprotection extents vs various irradiation times for the different resins after the exposure to femtosecond laser from the regenerative amplifier and post exposure bake. Lines are a guide to the eye.

possessed a slightly higher sensitizing efficiency and this result was opposite to that obtained in solution, where BDPO had a remarkably higher Φ_H than BDPA. It could be explained that the diffusions of the sensitizer and NIOTf in resin film were negligible, so the rate of electron transfer mainly depended on the energy rather than the lifetime of the excited state of the sensitizer. Consequently, the electron transfer process from excited singlet state would play an important role in the photoacid generation in resin film. BDPA, which has the higher fluorescence quantum yield and the larger 2PA cross-section, reasonably exhibited better sensitizing efficiency. As we expected, although resin E contained the same amount of NIOTf as resin R, there was no acid-catalyzed deprotection observed. Since resin R showed that even NIOTf itself can generate a small amount of acid upon exposure to femtosecond laser, this phenomenon gave evidence that the *N,N*-diethylaniline groups in BDEA actually bound the proton from the photoacid in the resin film. All of these results suggest that BDPA and BDPO can sensitize NIOTf to generate acid efficiently via 2PA and the triphenylamine group does not inhibit the acid-catalyzed chemical amplification.

3.6. Two-Photon Lithography. To demonstrate the potential of the developed two-photon acid generation systems in TPL, we fabricated micropatterns with resin A and O. In the presence of photoacid, a deprotective reaction converted the *t*-BOC-O-groups to phenolic hydroxyl groups and rendered the exposed material soluble in aqueous base developer. The final structure was obtained by dissolving the exposed resin in aqueous 0.26 M tetramethylammonium hydroxide after fabrication. In consistence with the chemical amplification measurements by 2PA, resins A and O exhibited comparable sensitivities and processabilities in TPL. Figure 8 shows the scanning electron microscope (SEM) images obtained using resin A and O. The 2D groove array (Figure 8a) was produced with resin O at a laser power of 0.24 mW and a scan speed of 10 μm s^{-1}. In comparison with the structures produced with negative photoresist based on free radical polymerization mechanism, the grooves showed low edge roughness. This implies that these photoresist systems have potential for high-fidelity TPL. In addition, parts b and c of Figure 8 present the intaglio text pattern and the spiral curve fabricated with resin A

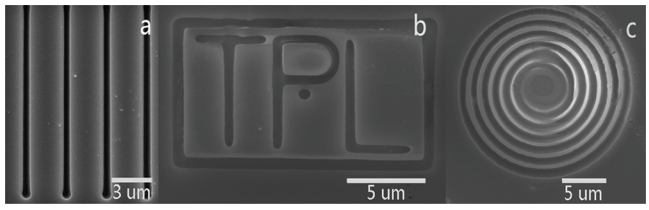

Figure 8. (a) SEM images of groove array fabricated with resin O at a laser power of 0.24 mW and a scan speed of 10 μm s^{-1}, (b) text pattern, and (c) spiral curve fabricated with resin A at a laser power of 0.5 mW and a scan speed of 110 μm s^{-1}.

at a laser power of 0.5 mW and a scan speed of 110 μm s^{-1}, respectively. The writing power of 0.24 mW is about 2 orders of magnitude smaller than that of the reported chemically amplified positive resist, which utilized ITX as the sensitizer.[22] This sensitivity is competitive with the previously reported results in high-sensitivity two-photon microfabrication, although this writing power is higher than the lowest value reported by Zhou et al.[3] Considering the greatly simplified preparation process, the results suggest that this two-photon chemically amplified positive resist is economic and efficient.

4. CONCLUSIONS

In this work, two 2PA dyes (BDPA and BDPO) containing triphenylamine as the electron donor have been synthesized by a facile route. In acetonitrile, BDPA and BDPO showed much higher two-photon absorption cross-section (σ > 1000 GM), compared with the conventional UV photoacid generators. They efficiently sensitized the commercially available nonionic PAG NIOTf via intermolecular electron transfer, which was induced by either one-photon or two-photon absorption. In acetonitrile solution, the quantum yield of photoacid generation for BDPO/NIOTf was measured to be as high as 0.053. The acid-catalyzed chemical amplification induced by 2PA in positive-tone resist film was confirmed by ATR-FTIR with the femtosecond laser from the regenerative amplifier, and both dyes exhibited remarkable sensitizing efficiency. This result proved that the triphenylamino group in the photosensitizer did not inhibit acid-catalyzed chemical amplification. Finally, TPL experiments were successfully carried out at a laser power as low as 0.24 mW. All the results suggest that the intermolecular photosensitization was an economic and practical method to build highly efficient photoacid generation system for two-photon chemically amplified positive resist.

■ ASSOCIATED CONTENT

Ⓢ Supporting Information

Measurements of the two-photon absorption cross-section and photoacid generation quantum yield. Cyclic voltammogram of BDPA and BDPO. Normalized absorption and emission spectra of BDPA and BDPO in PBOCS film. Logarithmic plots of 2PA induced fluorescence vs excitation power for BDPA and BDPO. This material is available free of charge via the Internet at http://pubs.acs.org.

■ AUTHOR INFORMATION

Corresponding Author

*Tel.: +86 10 82543569. Fax: +86 10 82543491. E-mail: fpwu@mail.ipc.ac.cn.

Notes

The authors declare no competing financial interest.

■ ACKNOWLEDGMENTS

This work was supported by the National Natural Science Foundation of China (No. 60978057). The authors are grateful to Dr. Xianzi Dong and Mr. Yanpeng Jia for their expertise assistance with the TPL experiments. They thank Dr. Yingquan Zou from Beijing Normal University for kindly providing polymer materials.

■ REFERENCES

(1) Kawata, S.; Sun, H.-B.; Tanaka, T.; Takada, K. *Nature* **2001**, *412*, 697−698.
(2) Cumpston, B. H.; Ananthavel, S. P.; Barlow, S.; Dyer, D. L.; Ehrlich, J. E.; Erskine, L. L.; Heikal, A. A.; Kuebler, S. M.; Lee, I.-Y. S.; Mccord-Maughon, D.; Qin, J.; Röckel, H.; Rumi, M.; Wu, X.-L.; Marder, S. R.; Perry, J. W. *Nature* **1999**, *398*, 51−54.
(3) Zhou, W.; Kuebler, S. M.; Braun, K. L.; Yu, T.; Cammack, J. K.; Ober, C. K.; Perry, J. W.; Marder, S. R. *Science* **2002**, *296*, 1106−1109.
(4) Parthenopoulos, D. A.; Rentzepis, P. M. *Science* **1989**, *245*, 843−845.
(5) Belfield, K. D.; Schafer, K. J. *Chem. Mater.* **2002**, *14*, 3656−3662.
(6) Bhawalkar, J. D.; Kumar, N. D.; Zhao, C.-F.; Prasad, P. N. *J. Clin. Laser Med. Surg.* **1997**, *15*, 201−204.
(7) Ogawa, K.; Kobuke, Y. *Anti-Cancer Agents Med. Chem.* **2008**, *8*, 269−279.
(8) So, P. T. C.; Dong, C. Y.; Masters, B. R.; Berland, K. M. *Annu. Rev. Biomed. Eng.* **2000**, *2*, 399−429.
(9) Larson, D. R.; Zipfel, W. R.; Williams, R. M.; Clark, S. W.; Bruchez, M. P.; Wise, F. W.; Webb, W. W. *Science* **2003**, *300*, 1434−1436.
(10) Ito, H. *Adv. Polym. Sci.* **2005**, *172*, 37−245.
(11) Moon, S.-Y.; Kim, J.-M. *J. Photochem. Photobiol., C* **2007**, *8*, 157−173.
(12) Reichmanis, E.; Houlihan, F. M.; Nalamasu, O.; Neenan, T. X. *Chem. Mater.* **1991**, *3*, 394−407.
(13) Yanez, C. O.; Andrade, C. D.; Belfield, K. D. *Chem. Commun.* **2009**, 827−829.
(14) Steidl, L.; Jhaveri, S. J.; Ayothi, R.; Sha, J.; Mcmullen, J. D.; Ng, S. Y. C.; Zipfel, W. R.; Zentel, R.; Ober, C. K. *J. Mater. Chem.* **2009**, *19*, 505−513.
(15) Li, C.; Luo, L.; Wang, S.; Huang, W.; Gong, Q.; Yang, Y.; Feng, S. *Chem. Phys. Lett.* **2001**, *340*, 444−448.
(16) Belfield, K. D.; Ren, X.; Van Stryland, E. W.; Hagan, D. J.; Dubikovsky, V.; Miesak, E. J. *J. Am. Chem. Soc.* **2000**, *122*, 1217−1218.
(17) Campagnola, P. J.; Delguidice, D. M.; Epling, G. A.; Hoffacker, K. D.; Howell, A. R.; Pitts, J. D.; Goodman, S. L. *Macromolecules* **2000**, *33*, 1511−1513.
(18) Boiko, Y.; Costa, J. M.; Wang, M.; Esener, S. *Opt. Express* **2001**, *8*, 517−584.
(19) Sha, J.; Lee, J.-K.; Kang, S.; Prabhu, V. M.; Soles, C. L.; Bonnesen, P. V.; Ober, C. K. *Chem. Mater.* **2010**, *22*, 3093−3098.
(20) Silva, A. D.; Sundberg, L. K.; Ito, H.; Sooriyakumaran, R.; Allen, R. D.; Ober, C. K. *Chem. Mater.* **2008**, *20*, 7292−7300.
(21) Vanderhart, D. L.; Prabhu, V. M.; Lin, E. K. *Chem. Mater.* **2004**, *16*, 3074−3084.
(22) Lee, J.-T.; George, M. C.; Moore, J. S.; Braun, P. V. *J. Am. Chem. Soc.* **2009**, *131*, 11294−11295.
(23) Schafer, K. J.; Hales, J. M.; Balu, M.; Belfield, K. D.; Van Stryland, E. W.; Hagan, D. J. *J. Photochem. Photobiol., A* **2004**, *162*, 497−502.
(24) Wu, J.; Zhao, Y.; Li, X.; Shi, M.; Wu, F.; Fang, X. *New J. Chem.* **2006**, *30*, 1098−1103.
(25) Guo, H.; Jiang, H.; Luo, L.; Wu, C.; Guo, H.; Wang, X.; Yang, H.; Gong, Q.; Wu, F.; Wang, T.; Shi, M. *Chem. Phys. Lett.* **2003**, *374*, 381−384.
(26) Xue, J.; Zhao, Y.; Wu, F.; Fang, D.-C. *J. Phys. Chem. A* **2010**, *114*, 5171−5179.
(27) March, J. *Advanced Organic Chemistry*. Wiley: New York, 1985.
(28) Lee, J. V. C. A. J. L. *Macromolecules* **1981**, *14*, 1141−1147.
(29) Ichimura, K.; Kameyama, A.; Hayashi, K. *J. Appl. Polym. Sci.* **1987**, *34*, 2747−2756.
(30) Narewska, J.; Strzelczyk, R.; Podsiadły, R. *J. Photochem. Photobiol., A* **2010**, *212*, 68−74.
(31) Renner, C. A. U.S. Patent 4,371,605, 1983.
(32) Hansen, M. M.; Riggs, J. R. *Tetrahedron Lett.* **1998**, *39*, 2705−2706.
(33) Wang, T.; Wu, F.; Shi, M.; Guo, H.; Wu, C.; Jiang, H.; Gong, Q. *Chem. Res. Chin. Univ.* **2003**, *19*, 470−473.
(34) Lee, H. J.; Sohn, J.; Hwang, J.; Park, S. Y. *Chem. Mater.* **2004**, *16*, 456−465.
(35) Demas, J. N.; Crosby, G. A. *J. Phys. Chem.* **1971**, *75*, 991−1024.
(36) Rehm, D.; Weller, A. *Isr. J. Chem.* **1970**, *8*, 259−271.
(37) Kavarnos, G. J.; Turro, N. J. *Chem. Rev.* **1986**, *86*, 401−449.
(38) Albota, M.; Beljonne, D.; Brédas, J.-L.; Ehrlich, J. E.; Fu, J.-Y.; Heikal, A. A.; Hess, S. E.; Kogej, T.; Levin, M. D.; Marder, S. R.; Mccord-Maughon, D.; Perry, J. W.; Röckel, H.; Rumi, M.; Subramaniam, G.; Webb, W. W.; Wu, X.-L.; Xu, C. *Science* **1998**, *281*, 1653−1656.
(39) Ortica, F.; Scaiano, J. C.; Pohlers, G.; Cameron, J. F.; Zampini, A. *Chem. Mater.* **2000**, *12*, 414−420.
(40) Suzuki, S.; Allonas, X.; Fouassier, J.-P.; Urano, T.; Takahara, S.; Yamaoka, T. *J. Photochem. Photobiol., A* **2006**, *181*, 60−66.
(41) Tarzi, O. I.; Allonas, X.; Ley, C.; Fouassier, J.-P. *J. Polym. Sci., Part A: Polym. Chem.* **2010**, *48*, 2594−2603.
(42) Fischer, A. B.; Bronstein-Bonte, I. *J. Photochem.* **1985**, *30*, 475−485.
(43) Guarr, T.; Mcguire, M.; Strauch, S.; Mclendon, G. *J. Am. Chem. Soc.* **1983**, *105*, 616−618.
(44) Miller, J. R.; Peeples, J. A.; Schmitt, M. J.; Closs, G. L. *J. Am. Chem. Soc.* **1982**, *104*, 6488−6493.